AIMS Molecular Science, 3(1): 32-51.
DOI: 10.3934/molsci.2016.1.32
Received 30 October 2015,
Accepted 01 February 2016,
Published 16 February 2016

http://www.aimspress.com/journal/Molecular

Research article

The aliphatic counterpart of PET, PPT and PBT aromatic polyesters: effect of the molecular structure on thermo-mechanical properties

Morgane Albanese, Justine Boyenval, Paola Marchese, Simone Sullalti and Annamaria Celli *

Department of Civil, Chemical, Environmental and Materials Engineering, University of Bologna, Via Terracini 28, BO 40131, Italy

* **Correspondence:** Email: annamaria.celli@unibo.it; Tel: +39-051-209-0349; Fax: +39-051-209-0322.

Abstract: The aliphatic counterparts of the most used aromatic polyesters (PET, PPT, and PBT) have been synthesized by a two-stage polycondensation process, starting from dimethyl 1,4-cyclohexane dicarboxylate and different diols. The fully aliphatic polyesters are characterized by two cis/trans isomeric ratios (50 and 90 mol%) of the 1,4-cycloaliphatic rings. According to the cis/trans content, the properties of the materials notably change. Indeed, polymers rich in trans isomer are semicrystalline, whereas polymers with low trans content are fully amorphous, due to the presence of kinks along the chain. Trans isomer is characterized by higher rigidity than the cis one and the corresponding polymers have high glass transition temperatures. Moreover, the length of the methylene sequences in the diol has a notable influence on the final thermal and mechanical properties. Therefore, tunable properties can be easily obtained. This characteristic, in association with good mechanical performances, potential sustainability of the monomers and biodegradability, makes these aliphatic polyesters an interesting class of polyesters for some specific applications.

Keywords: Polyesters; 1,4-cyclohexylene ring; cis/trans ratio; thermal properties; crystallization kinetics

1. Introduction

Bio-based and biodegradable polymers are continuously object of a great interest from academy and industry due to the necessity to substitute traditional plastics derived from not-renewable resources and often resistant to degradation with new materials obtained from biomass and

environmentally friendly [1,4]. In particular, notable efforts are nowadays evident to find new solutions for the substitution of important aromatic polyesters, such as poly(ethylene terephthalate) (PET), poly(propylene terephthalate) (PPT), and poly(butylene terephthalate) (PBT), which cover a significant market of plastics in Europe, due to their excellent thermal and mechanical properties, low permeability, chemical resistance, and low costs. In particular, PET is the sixth more requested polymers in Europe, with a demand of 3000 ktonne in 2012, and is used in bottle containers, food packaging, textile fibers, engineering plastics and electronics [5].

The diols used to produce PET, PPT and PBT, i.e. 1,2-ethanediol, 1,3 propanediol, and 1,4 butanediol (BD), are now available by new routes from biobased resources [6]. On the other hand, for the production of terephthalic acid (TPA) from renewable resources, some green pathways have been developed [6], for example by starting from terpenes [7], thought a really convenient route from an industrial point of view has not yet been found. For this reason, also sustainable substitutes of terephthalic acid have been proposed, such as 2,5-furandicarboxylic acid, ferulic acid, and vanillic acid [8-12].

Another possible building block, alternative to terephthalic acid, is the 1,4-cyclohexanedicarboxylic acid (CHDA). It is exactly the aliphatic counterpart of the aromatic TPA and can be prepared from bio-based terephthalic acid, starting from limonene and other terpenes [13]. Moreover, CHDA or its dimethyl ester (dimethyl 1,4-cyclohexanedicarboxylate, DMCD) present some further advantages with respect to TPA as monomer in polyester synthesis. Firstly, aliphatic-alicyclic copolymers resulted to have a significantly high biodegradability, notably larger than that of similar copolymers containing terephtahlic units [14-16]. Moreover, the polymers derived from CHDA or DMCD can be prepared by modulating the amount of the cis and trans isomers of the 1,4-cycloaliphatic rings (see Scheme 1). The corresponding final properties strongly vary according to the cis/trans ratio, the trans isomer being less flexible and more symmetrical than the cis stereoisomer. Highly symmetrical units improve chain packing with a consequent increment in crystalline perfection. Therefore, polymers characterized by high trans content of the aliphatic ring are semicrystalline with melting temperature that increases with the increment of the trans percentage. On the other hand, polymers containing high amount of cis isomer are fully amorphous. Therefore, the final properties of the polymers containing 1,4-cycloaliphatic rings can be easily tailored according to the specific applications. This phase behaviour has been deeply studied for polymers such as poly(butylene 1,4-cyclohexanedicarboxylate, PBCHD) and poly(1,4-cyclohexylenedimethylene 1,4-cyclohexanedicarboxylate, PCCD) by the Authors [17-20], other polymers containing 1,4-cyclohexylene rings have been also recently described in literature [21-24].

trans configuration cis configuration

Scheme 1. Trans and cis configurations of CHDA unit.

For all these reasons, the use of CHDA or DMCD to prepare the aliphatic counterpart of PET, PPT, and PBT polyesters is a very attracting topic. Therefore, this work focuses on the synthesis and characterization of poly(ethylene 1,4-cyclohexanedicarboxylate) (PECHD) and poly(propylene 1,4-cyclohexanedicarboxylate) (PPCHD) (Scheme 2), with different cis/trans molar ratio (50/50 and 10/90 mol%). Some data concerning of PBCHD, already published, have been also used to discuss correlations existing between chemical structure and material properties. Moreover, the properties of these aliphatic polyesters are compared with those of PET, PPT, and PBT.

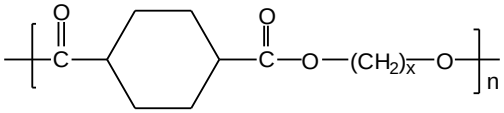

X = 2, 3, 4

Scheme 2. Molecular structure of the aliphatic polyesters

2. Materials and Method

2.1. Materials

Two commercial samples of DMCD with 22% and 100% of trans isomer content, 1,2-ethanediol, 1,3-propanediol, 1,4-butanediol, and titanium tetrabutoxide (TBT) (all from Aldrich chemicals) were high purity products, used as received. PET, PPT and PBT were previously prepared in our laboratory according to the procedure described in reference [25] (for PET), [26] (for PPT), and [27] for PBT.

2.2. Synthesis of polyesters

The aliphatic polyester samples were synthesised in a two-stage process, from dimethyl 1,4-cyclohexane dicarboxylate (DMCD) with two different ratios of cis/trans and different diols (1,2-ethanediol, 1,3-propanediol, 1,4-butanediol). The different percentages of the trans isomer of the cyclohexylene ring (90 and 50 mol%) were obtained by a convenient mixture of two DMCD monomers, 100 and 22 mol % of trans.

The samples are named with the code $PxCHD_y$ where x is a letter indicating the diol used (E = 1,2-ethanediol, P = 1,3-propanediol, B = 1,4-butanediol) and y is the percentage of the aliphatic rings, derived from DMCD, in trans configuration. The aromatic samples are indicated with the PxT code, where also in this case x is the letter indicating the diol monomeric structure.

The syntheses were performed in accordance with the procedure described in reference [17]. As an example, the synthesis of $PPCHD_{90}$ is here described.

DMCD 100 mol% trans (26.15 g, 0.131 mol), DMCD 22 mol% trans (3.85 g, 0.019 mol), (1,3-propanediol (15.96 g, 0.210 mol) and TBT (0.04 g, 0.12 mmol) were placed into a round-bottomed wide-neck glass reactor (250 mL capacity). The reactor was closed with a three-neck flat flange lid equipped with a mechanical stirrer and a torque meter that gives an indication of the viscosity of the reaction melt. The reactor was immersed into a salt bath preheated to 200 °C. The first stage was conducted at atmospheric pressure under nitrogen atmosphere and the mixture was

allowed to react during 120 minutes under stirring with continuous removal of methanol. The second stage was started to gradually decreasing the pressure to 0.4 mbar while the temperature was raised to the final temperature of 220 °C. These conditions were reached within 60 minutes, using a linear gradient of temperature and pressure, and maintained during 180 minutes.

Before investigation, PxT and $PxCHD_{90}$ samples were purified. PxT samples were dissolved in a mixture of chloroform/1,1,1,3,3,3-hexafluoro-2-propanol (HFIP) (90/10 vol%) and precipitated in methanol; $PxCHD_{90}$ samples were dissolved in chloroform and precipitated in methanol.

2.3. Characterization

The ^{1}H NMR spectra of $PxCHD_y$ samples were recorded at room temperature on samples dissolved in $CDCl_3$ using Varian Mercury 400 spectrometer, the proton frequency being 400 MHz. Chemical shifts are in part per million (ppm) down-field from TMS.

Molecular weights (expressed in equivalent polystyrene) were determined by gel permeation chromatography (GPC) using a HP Series 1100 liquid chromatography instrument equipped with a PL gel 5μ Mixed-C column and refractive index as detector. Chloroform/HFIP (98/2 vol%) mixture was used as eluent for PxT samples and chloroform for $PxCHD_y$ samples.

Thermogravimetric analysis was performed using a Perkin-Elmer TGA7 thermobalance under nitrogen atmosphere (gas flow 40 $mL \cdot min^{-1}$) at 10 $°C \cdot min^{-1}$ heating rate from 40 °C to 900 °C. The temperature of the maximum degradation rate (T_D), corresponding to the maximum of the differential thermogravimetric curve, was calculated.

ATR FT-IR analysis was conducted over the wavenumber range 650–4000 cm^{-1} using a Perkin Elmer Spectrum One FT-IR spectrometer equipped with a Universal ATR Sampling accessory. Before analysis, some samples were prepared in Differential Scanning Calorimetry (DSC) with the following thermal treatments: first heating scan at 20 $°C \cdot min^{-1}$ to a temperature 40 °C higher than melting peak, in order to completely melt the polymer, and cooling scan at different rates to obtain polymers with different crystallization degree.

The wide angle X-ray scattering (WAXS) data were collected with X'PertPro diffractometer equipped with a copper anode (Kα radiation, λ = 1.5418 Å). The data were collected in the 2θ range of 5–60° by means of X'Celerator detector. The measurements were performed on samples prepared in DSC with the following thermal treatment: first heating scan at 20 $°C \cdot min^{-1}$ to a temperature 40 °C higher than the melting peak, in order to completely melt the polymer, and cooling scan at 1 $°C \cdot min^{-1}$ to 20 °C.

The calorimetric analysis was carried out by means of a Perkin-Elmer DSC6 for measurements in non-isothermal conditions and by means of a Perkin-Elmer DSC7, equipped with a liquid sub ambient accessory, for measurements in isothermal conditions. High purity standards were used in calibrating the instrument and measurements were performed under nitrogen flow (gas flow 20 $mL \cdot min^{-1}$)

In non-isothermal analysis, the samples (5–10 mg) were heated at 20 $°C \cdot min^{-1}$ to different temperatures varying from 180 to 280 °C, chosen 40 °C higher than the melting peak of each sample, in order to cancel the previous thermal history, kept at this temperature for 1 min and then cooled to −40 °C at 10 $°C \cdot min^{-1}$. After this thermal treatment, the sample were analyzed by heating to 180–280 °C at 10 $°C \cdot min^{-1}$ (2nd scan). During the cooling scan, crystallization temperature (Tc) and enthalpy of crystallisation (ΔHc) were measured. During the 2nd scan the glass transition temperature

(*T*g), the eventual cold crystallization temperature (*T*cc) and enthalpy (Δ*H*cc), the melting temperature (*T*m) and enthalpy of fusion (Δ*H*m) were determined.

Isothermal crystallization experiments were carried out on $PxCHD_{90}$ as follows: melting at 185–200 °C (at about a temperature 40 °C higher than *T*m) according to the sample characteristics, holding for 1 min at this temperature, fast cooling to the selected crystallization temperature *T*c, isotherm at *T*c long enough to complete the crystallization process and heating at 10 °C·min^{-1} in order to observe the melting process.

Samples for dynamic mechanical measurements were obtained by injection molding in a Mini Mix Molder (Custom Scientific Instruments) equipped with a rectangular mold (30 × 8 × 1.6 mm). The molded samples were rapidly cooled in water and then dried in an oven at 50 °C under vacuum overnight. Dynamic mechanical measurements were performed with a dynamic mechanical thermal analyzer (Rheometrics Scientific, DMTA IV), operated in the dual cantilever bending mode, at a frequency of 3 Hz and a heating rate of 3 °C·min^{-1}, over a temperature range from −120 °C to a final temperature varying from 100 to 150 °C, according to the sample characteristics.

3. Results and Discussion

3.1. Molecular characterization

The synthetic procedure used to prepare the aliphatic $PxCHD_y$ polyesters is a traditional two-step polycondensation carried out in the presence of a catalyst. As reported in the experimental part, by starting from an adequate physical mixture of the two components it is possible to obtain polymers with the desired final stereochemistry of the aliphatic rings. Here, for each polymer, two trans contents have been chosen, 50 and 90 mol%, as reported in Table 1. These two different percentages enable us to have different thermal properties of the materials.

Table 1. Trans percentage in the cyclohexylene units, molecular weight (*M*w) and molecular weight distribution (*M*w/*M*n) for $PxCHD_y$ and PxT samples.

Samples	Trans % of the ring in the polymer [a)]	$M_w \times 10^{-3}$ [b)]	M_w/M_n [b)]
$PECHD_{50}$	53	84.1	2.5
$PPCHD_{50}$	53	62.4	2.4
$PBCHD_{50}$	52	88.6	2.8
$PECHD_{90}$	87	85.6	2.5
$PPCHD_{90}$	87	65.6	2.5
$PBCHD_{90}$	91	54.9	2.3
PET	-	55.0	2.4
PPT	-	60.7	2.8
PBT	-	110.0	2.6

[a)] Calculated by ^{1}H NMR ; [b)] Measured by GPC in $CHCl_3$ for PxCHD samples and in $CHCl_3$/HFIP (98/2 vol%) mixture for PxT samples.

Proton NMR analyses were carried out in order to check the molecular structure and the cis/trans isomeric ratio of the aliphatic samples. As an example, Figure 1 shows the ^{1}H NMR spectrum of the $PECHD_{90}$ sample, where the signal assignation is reported. The molecular structure

is confirmed. The same result has been obtained for all the aliphatic samples (spectra not shown). For $PECHD_{90}$ it is notable that the signals due to the chain ends are visible in the insert of Figure 1 together with the signals due to the presence of a small amount of diethylene glycol units ($O{-}CH_2{-}CH_2{-}O{-}CH_2{-}CH_2{-}O{-}$) (DEG) in the polymer chain. An estimation of their amount indicates that the DEG percentage is about 2 mol%. Minor amounts (≤3%) of DEG units are commonly found in ethylene glycol based polyesters, such as PET, where they appear as a consequence of etherification side reactions taking place during the transesterification step. The presence of such units is known to have deleterious effects on thermal transition temperatures of the polyester [28-29].

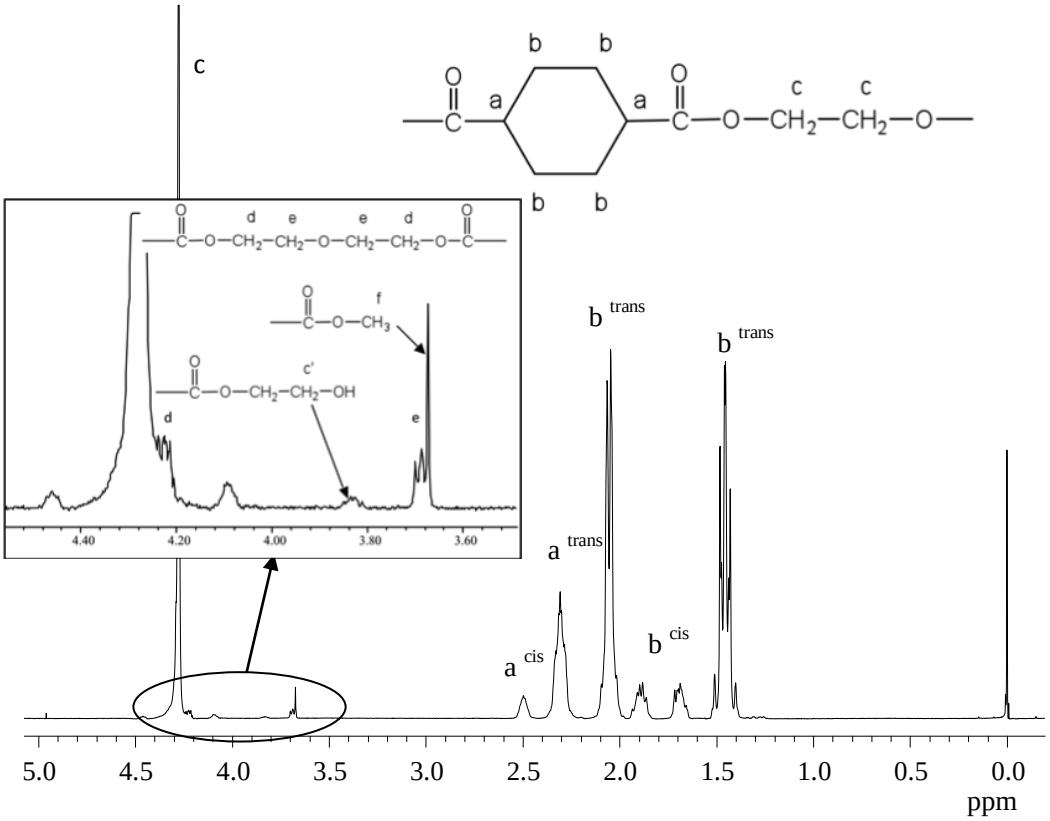

Figure 1. ^{1}H NMR spectrum of $PECHD_{90}$ sample with H assignation.

The trans and cis signals appear in the range of 1.3–2.6 ppm and are clearly resolvable. The ratio of the areas of the signals centered at 2.3 (trans isomer) and 2.5 (cis isomer) ppm has been used to calculate the trans percentage, according to the procedure described in ref. 17. Moreover, the NMR analysis confirms that no isomerization from trans to cis form occurs at the conditions used for the polymerization process. Indeed, the 1,4-cyclohexylene ring could isomerize towards the thermodinamically stable cis/trans ratio equal to 34/66, during polymer synthesis, if an acid environment is present or during thermal treatments carried out at temperatures higher than 260 °C and for longer than 1 h [30]. These conditions are not present in the polymerization medium.

The possibility of distinguishing between cis and trans isomers is investigated also by using ATR-FTIR analysis. The literature does not report clear indications about this topic. Firstly, the effect of the crystallinity has been evaluated: the analyses carried out on the same sample with different

degrees of crystallinity, obtained by different cooling rates from the melt in DSC, do not show any changes in the spectra. Therefore, it is possible to neglect the effect of different degrees of crystallinity in FTIR analysis.

Figure 2 shows the ATR-FTIR spectra recorded for $PPCHD_{90}$ and $PPCHD_{50}$, analysed as obtained.

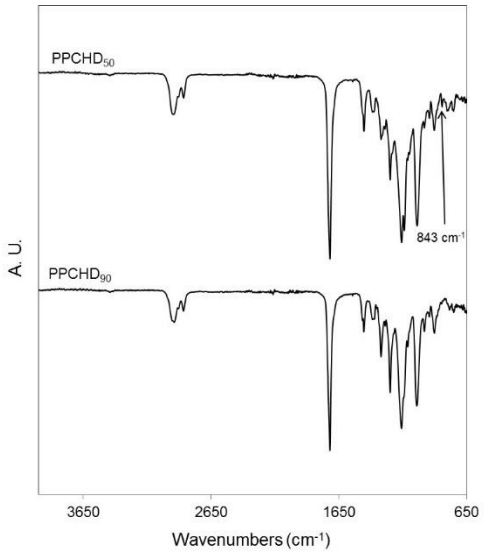

Figure 2. ATR-FTIR spectra of $PPCHD_{90}$ and $PPCHD_{50}$.

Typical bands attributed to the aliphatic C-H stretch at 2940–2870 cm^{-1} and -CH_2 bending band at 1450 cm^{-1} are present. The strong carbonyl absorbance at 1720 cm^{-1} is evident as well as the absorbance due to the C-O bond centred at 1040 cm^{-1} and 1160 cm^{-1}. By a careful comparison between the two spectra it is noteworthy that the spectrum of the specimen with the highest cis content ($PPCHD_{50}$) presents a band at 843 cm^{-1} which does not exist in the corresponding $PPCHD_{90}$ spectrum. The same result has been obtained by carefully checking the spectra obtained for the PECHDy and PBCHDy samples. Therefore, it is possible to hypothesize that the peak at 843 cm^{-1} is due to the cis isomer in the $PxCHD_{50}$ samples. A similar result has been obtained in [31].

Concerning the molecular weights reported in Table 1, it is evident that all the aliphatic polyesters have high and similar *M*w and, then, can be suitable for a comparison in terms of thermal behavior.

3.2. Thermogravimetric analysis

Thermal stability of the samples was analyzed using TGA in nitrogen atmosphere. As visible in Figure 3, the aliphatic polyesters have a notable stability, as the degradation process begins above 320 °C. It occurs in a single step up to a complete weight loss. The temperatures of the maximum degradation rate (T_D), reported in Table 2, confirm this behaviour for all the $PxCHD_y$s. Moreover, the results exclude also an influence of the stereochemistry of the aliphatic ring on the stability of the polymers, as already observed for other polyesters containing the 1,4-cycloaliphatic units [18].

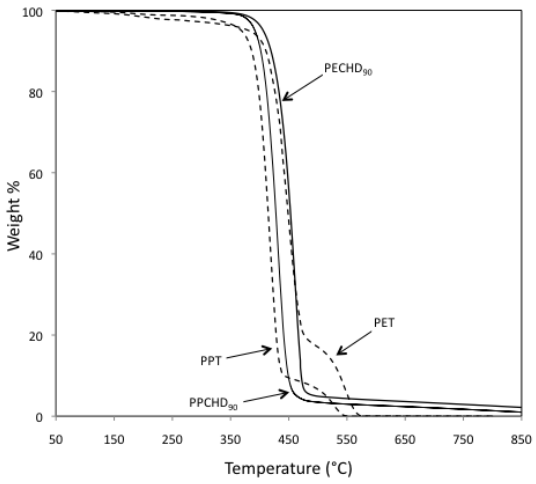

Figure 3. Thermogravimetric curves obtained in nitrogen at 10 °C·min^{-1} of PET, PECHD$_{90}$, PPT and PPCHD$_{90}$ samples.

Table 2. Thermal data for PxCHD$_y$ and PxT samples.

Samples	T_D [a] (°C)	Tc [b] (°C)	ΔHc [b] (J·g^{-1})	Tg [c] (°C)	Tcc [c] (°C)	ΔHcc [c] (J·g^{-1})	Tm [c] (°C)	ΔHm [c] (J·g^{-1})	Tm^o [d] (°C)
PECHD$_{50}$	460	-	-	14	-	-	-	-	-
PPCHD$_{50}$	431	-	-	−1	-	-	-	-	-
PBCHD$_{50}$	433	-	-	−9	-	-	-	-	-
PECHD$_{90}$	462	-	-	24	113	3	145	4	Nd [e]
PPCHD$_{90}$	432	71	19	7	67	11	140	29	152
PBCHD$_{90}$	433	132	43	5	-	-	150–158	46	170
PET	451	188	34	82	-	-	254	31	272
PPT	418	174	47	54	-	-	230	54	241
PBT	408	192	57	42	-	-	217–223	55	233

[a] Temperature of the maximum degradation rate measured in TGA under nitrogen flow at 10 °C·min^{-1}; [b] Measured in DSC during the cooling scan at 10 °C·min^{-1}; [c] Measured in DSC during the second heating scan at 10 °C·min^{-1}; [d] calculated by Hoffmann-Weeks equation; [e] not determined.

By comparing aliphatic materials with the corresponding aromatic polymers, it is evident that the 1,4-cyclohexylene units improve the thermal stability of the materials with respect to the terephthalate units. The same observations have been made, for example, by Wang et al. [32] for copolymers based on PET: the introduction of C_6 aliphatic rings increases the thermal stability of PET of 5–10 degrees, accordingly to the 1,4-cyclohexylene unit content. Moreover, also the substitution of the butylene units in PBCHD with another aliphatic ring, in PCCD, contribute to further stabilize the material [33].

In a similar way, the thermal stability of some aliphatic-aromatic random copolyesters increases as the cyclic units, obtained from CHDM, increase [34].

Finally, it is noteworthy that polyesters derived from ethanediol (PECHD and PET) present T_D values notable higher with respect to the T_D values of the other aliphatic and aromatic specimens, respectively (PECHD 460–462 °C vs PPCHD 431–432 and PBCHD 433 °C; PET 451 vs PPT 418

and PBT 408 °C). The higher thermal stability of PET with respect to PPT and PBT has been already observed in literature and attributed to the different stability of the end groups created after chain cleavage [35]. The instability of the vinyl endgroups in PET results in a net loss of glycol units, which improves the equilibrium stoichiometry during degradation. This provides a competing, productive mechanism that partially compensates for the decrease in conversion by chain cleavage. On the other hand, in PTT and PBT allyl and butenyl are relatively stable chain-terminating endgroups and the overall stoichiometry does not change as a result of thermal chain cleavage. The same behaviour can be imputed to the PECHDs with respect to PPCHD and PBCHD samples.

3.3. Influence of stereochemistry and aliphatic chain length on thermal behavior

Figure 4–6 show the DSC curves of the cooling and second heating scans of the $PxCHD_y$ samples, together with those of PxT specimens. All the DSC data are collected in Table 2.

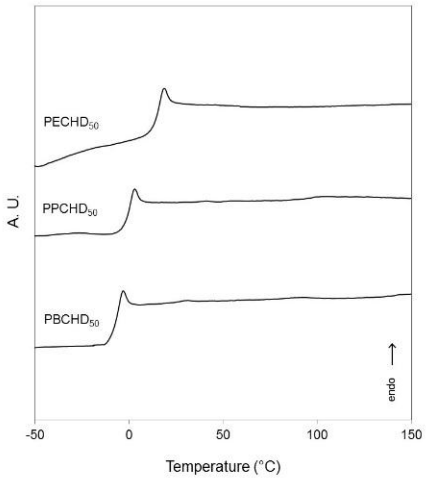

Figure 4. DSC traces obtained on $PxCHD_{50}$ samples during the second heating scan.

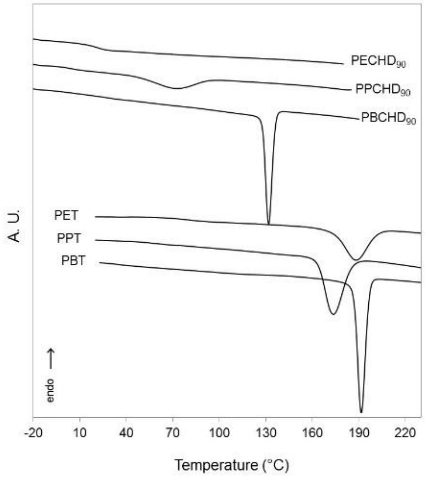

Figure 5. DSC traces obtained on $PxCHD_{90}$ and PxT samples during the cooling scan.

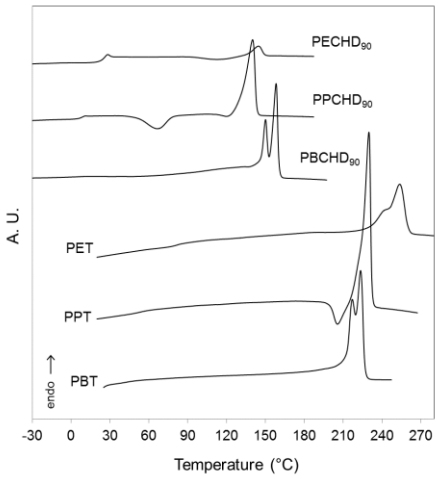

Figure 6. DSC traces obtained on $PxCHD_{90}$ and PxT samples during the second heating scan.

By considering the second heating scans of the $PxCHD_{50}$ specimens (Figure 4), it is noteworthy that these samples are fully amorphous, whereas the $PxCHD_{90}$ specimens (Figure 5–6), mainly $PPCHD_{90}$ and $PBCHD_{90}$, are able to crystallize. This behaviour confirms that the trans configuration of the aliphatic C_6 rings improves the capacity of the samples to reach an ordered state. Indeed in the preferred chain conformation of the 1,4-cyclohexylene units, the trans configuration is more stretched and symmetrical than cis one, thus suitable for good chain packing. The cis configuration, instead, introduces non-linear moieties and kinks along the main chain, which result to hinder formation of stable and perfect crystals [17,19,33].

Concerning the amorphous phase, PxCHD samples have *T*g values located in the range from −9 to 24 °C. From Table 2 and Figure 7a it is notable that $PxCHD_{50}$ samples are characterized by glass transition temperatures that are about 10 °C lower than those of $PxCHD_{90}$ specimens. As an example, PBCHD has a *T*g of −9 °C when contains 50 mol% of trans isomer and a *T*g of 5 °C when the trans amount increases to 90 mol%. The higher *T*g values in the $PBCHD_{90}$ series can be due to the presence of a high amount of trans isomer, more rigid than the cis one, and to the crystallinity, mainly for $PPCHD_{90}$ and $PBCHD_{90}$ samples. Both factors, trans isomer and crystallinity, contribute to increment the rigidity of the chains and to increase the glass transition temperature. Finally, it is notable that *T*g decreases with the lengthening of the aliphatic chain, as in PxT series, due to a larger flexibility of a longer methylene sequence.

Concerning the crystalline phase, for $PxCHD_{90}$ series it is noteworthy (Figure 5, 6) that the sample containing a short aliphatic chain (a sequence of 2 methylene units in $PECHD_{90}$) is characterized by a very low crystallinity, when analyzed in DSC at 10 °C·min^{-1} of cooling and heating rates. An analogous trend is evident by comparing crystallization enthalpies of PET with those of PPT and PBT. On the other hand, $PPCHD_{90}$ specimen crystallizes partially during the cooling scan and completes its crystallization during the second heating scan, indicating a relatively slow crystallization rate. This behaviour is confirmed in Figure 7b, where the *T*c datum for $PPCHD_{90}$ is very low. $PBCHD_{90}$, instead, crystallizes only during the cooling scan, suggesting a higher capability in reaching an ordered state. Therefore, it is evident that in the $PxCHD_{90}$ series the length of the aliphatic chain strongly influences the crystallization rate and degree of crystallinity, which

increase with the lengthening of the $–CH_2-$ sequences. These differences in ability to crystallize are not so evident for the PxT series (Figure 5). Moreover, the difficulty in crystallizing of $PECHD_{90}$ could be due also to the presence of DEG units that cause a decrement of the crystallization rate, as observed for PET [29]. However, when slower cooling rate are used (1 °C·min^{-1}), also the $PECHD_{90}$ specimen is able to reach a significant level of crystallinity, as reported in Table 3.

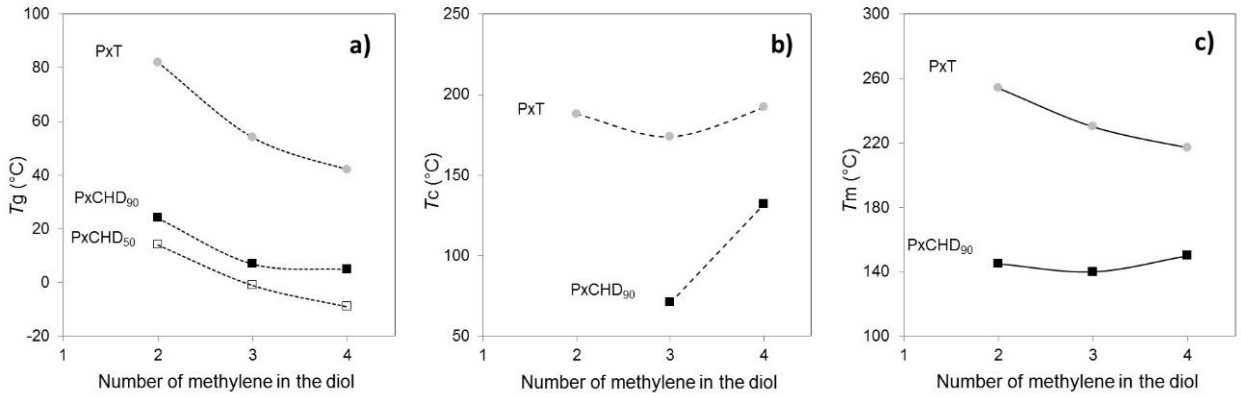

Figure 7. Trend of *T*g (Figure 7a), *T*cc (Figure 7b) and *T*m (Figure 7c) as a function of the number of methylene groups in the aliphatic chain of $PxCHD_y$ and PxT series.

Table 3. DSC data for $PxCHD_{90}$ samples cooled at 1 °C/min.

Samples	*T*c[a] (°C)	Δ*H*c[a] (J·g^{-1})	*T*g[b] (°C)	*T*cc[b] (°C)	Δ*H*cc[b] (J·g^{-1})	*T*m[b] (°C)	Δ*H*m[b] (J·g^{-1})
$PECHD_{90}$	91	23	27	-	-	143	23
$PPCHD_{90}$	101	41	11	-	-	130–141	41
$PBCHD_{90}$	142	42	-	-	-	155	42

[a] Measured in DSC during the cooling scan at 1 °C·min^{-1}; [b] Measured in DSC during the second heating scan at 10 °C·min^{-1}.

From Figure 6 it is also visible that $PBCHD_{90}$ presents multiple and complex melting processes that have been attributed to melting-recrystallization-remelting processes occurring during the calorimetric scan [17]. The same behaviour takes place in PBT in the analysis at 10 °C·min^{-1}. This is typical of the polymers, especially polyesters that are characterized by a relatively high crystallization rate and can rearrange their crystalline state along the DSC scan. In any case, due to this complex melting behavior, it should be emphasized that the Δ*H*m given in Table 2 are only indicative because they do not refer to a simply melting phenomenon.

Figure 7 can be also useful to compare the thermal behaviour of $PxCHD_y$ samples with their aromatic counterparts. It is important to notice that glass transitions of aromatic polyesters are considerably higher than those of the corresponding aliphatic polyesters (Figure 7a). As an example, PBT has a *T*g of 42 °C, which is about 40 °C higher than the *T*g of the semicrystalline and amorphous PBCHDs (*T*g = 5 and −9 °C, respectively). The same behavior is visible for PET and PPT with respect to the aliphatic counterparts. Moreover, it is notable that aromatic polyesters are characterized by very high values of the *T*c and *T*m (Figure 7b and 7c). All these differences can be justified by considering that in polyesters based on terephthalic acid, the coplanarity between the

carbonyl and phenyl groups restricts the rotational angles about C_{phenyl}-CO to 0 and 180 °, even if rotations about the terephthaloyl residue virtual bond, resulting in nonplanar conformations, are also probable, with a barrier which increases for rotation angles increasing from 0 to 90 ° [36-38]. The planar conformation favors the molecular packing of the chains in the crystal, and enhances the attractive intermolecular interactions between the ester groups of neighboring chains. As a result, the aromatic polyesters exhibit high melting points [38]. The low flexibility of the chains, moreover, induces a high *T*g value. On the other hand, in PxCHD the presence of the aliphatic ring, in chair or boat conformations, excludes the planarity of the CO-C_6 system; moreover the cyclohexyl groups are conformationally more mobile than the rigid phenyl ring. For these reasons the melting temperatures and *T*g values are considerably lower [39].

In order to better understand the crystallization behaviour, the X-ray diffraction analysis has been performed on the $PxCHD_{90}$ samples, cooled from the melt at 1 °C·min^{-1} in DSC. Figure 8 shows the spectra where it is notable a high level of crystallinity for all the samples and the presence of three different crystalline phases, depending on the chain length of the diol. A more in depth study on these different crystalline phases could justify the trend of melting temperatures reported in Figure 7c.

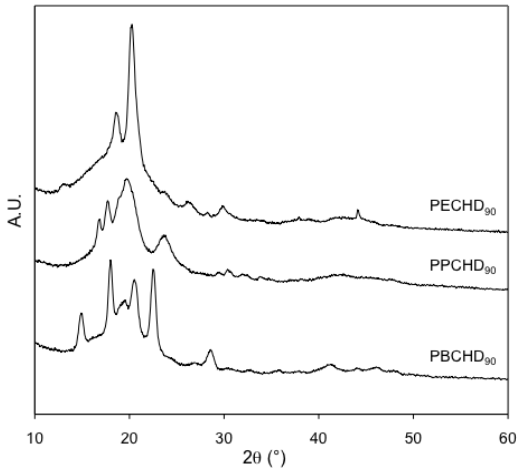

Figure 8. WAXD analysis carried out on $PxCHD_{90}$ samples non-isothermally crystallized in DSC (cooling from the melt at 1 °C·min^{-1}).

As a conclusion, PxCHD samples can be prepared in amorphous or semicrystalline state, according to the cis/trans ratio of the cyclohexylene rings present along the chain. They are characterized by *T*g and *T*m values notably lower than those of their aromatic counterparts (about 60 and 100 °C lower, respectively), due to differences in chemical structure of the aliphatic and aromatic rings.

3.4. Isothermal crystallization

The crystallization processes of the $PxCHD_{90}$ samples have been studied in isothermal conditions, in order to better understand their phase behaviour and to obtain some kinetic parameters. This study was performed on purified samples to eliminate impurities that can strongly influence the

crystallization process. $PPCHD_{90}$ and $PBCHD_{90}$ present the ability of crystallizing in isothermal conditions, whereas $PECHD_{90}$ is characterized by a crystallization rate that is too slow in the temperature range analysed. The crystallization temperatures (*T*c), chosen according to the polymer characteristics, are reported in Table 4.

Table 4. Results of the isothermal crystallization analysis for $PxCHD_{90}$ and PxT samples: crystallization temperature (*T*c), half-time of crystallization ($t_{1/2}$), Avrami exponent (*n*) and Avrami constant (*k*).

Samples	*T*c (°C)	$t_{1/2}$ (s)	*n*	*k* (s^{-n})
$PPCHD_{90}$	96	236	2.3	1.8×10^{-6}
	98	265	2.3	2.5×10^{-6}
	100	319	2.4	7.6×10^{-7}
	102	380	2.3	1.1×10^{-6}
	104	462	2.4	5.3×10^{-7}
$PBCHD_{90}$	138	80	3.0	1.5×10^{-6}
	140	112	2.7	1.9×10^{-6}
	142	180	2.6	7.5×10^{-7}
	144	280	2.7	1.9×10^{-7}
	146	604	2.9	8.4×10^{-9}
PET	201	299	2.1	4.6×10^{-6}
	203	325	2.0	7.5×10^{-6}
	205	460	2.2	1.1×10^{-6}
	207	480	2.2	5.0×10^{-6}
	210	544	2.0	3.4×10^{-6}
PPT	191	102	2.3	2.0×10^{-5}
	193	122	2.2	1.7×10^{-5}
	195	258	2.1	6.3×10^{-6}
	197	433	2.4	4.0×10^{-7}
	199	551	2.5	1.2×10^{-7}
PBT	196	72	2.6	1.2×10^{-5}
	198	116	2.5	5.1×10^{-6}
	200	219	2.4	1.4×10^{-6}
	202	310	2.6	2.4×10^{-7}
	204	649	2.6	2.7×10^{-8}

Figure 9 shows some typical calorimetric traces of the $PxCHD_y$ samples that were isothermally crystallized at different temperatures (*T*c) and subsequently melted. As discussed for PBCHD in [20], during the heating scan multiple and complex melting processes occur, which are typical of polyesters [40]. Peak I can be associated with the melting of the poorer crystal grew at Tc, peak II can be ascribed to the fusion of crystal actually formed at *T*c. Peak III can be explained as due to the melting of the most perfect crystals grown through melting-recrystallization processes. From the analysis of the melting processes, it is possible to extrapolate the *T*m° value, which is the equilibrium melting temperature, i.e. the melting temperature of perfect lamellar crystals with an infinite tickness. These data are crucial in order to compare the crystallization rates of the different samples in similar

conditions, i.e. at the same undercooling $\Delta T = T\text{m}° - T\text{c}$. Among the most commonly used procedures to evaluate $T\text{m}°$, the Hoffmann-Weeks method is especially acceptable thanks to its simplicity, through the relationship [41]:

$$T_\text{m} = T_\text{m}^\circ \left(1 - \frac{1}{\gamma}\right) + \frac{T_\text{C}}{\gamma} \qquad (1)$$

where $T\text{m}$ is the experimental melting temperature and γ is a factor depending on the lamellar thickness. $T\text{m}°$ can be obtained from the crossing point of the $T\text{m} = T\text{c}$ line with the extrapolated $T\text{m}$ vs $T\text{c}$ line. The extrapolated values of $T\text{m}°$ are reported in Table 2: they are equal to 152 and 170 °C for $PPCHD_{90}$ and $PBCHD_{90}$, respectively. For the aromatic samples the obtained data are in agreement with the literature [42].

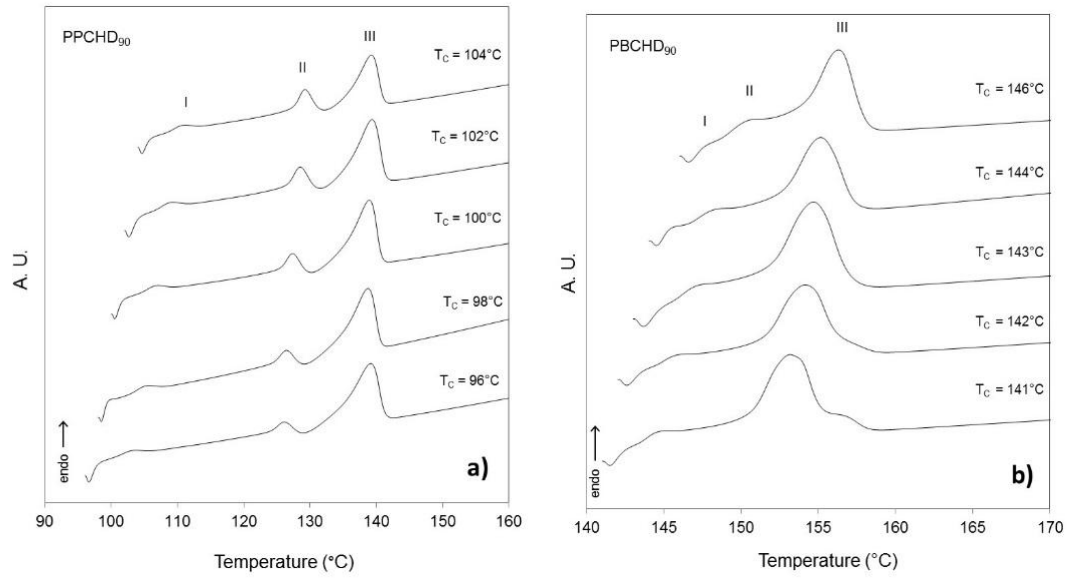

Figure 9. Melting endotherms obtained by DSC on $PECHD_{90}$ (a) and $PBCHD_{90}$ (b) samples after isothermal crystallization at the $T\text{c}$ indicated on the curves.

The overall crystallization process has been analyzed by considering the isothermal curves, which report heat flow as a function of time. They were analyzed by the Avrami equation [43-45]:

$$X_\text{t} = 1 - exp[-k(t - t_0)^n] \qquad (2)$$

where X_t is the crystalline fraction, as calculated from the ratio of the area of the exothermal peak in the thermogram at the time $t\text{c}$ and the total area of the crystallization process. k is the overall kinetic constant, t_0 is the induction time, i.e. the time span before crystallization begins at the isothermal crystallization temperature $T\text{c}$. n is an exponent whose value depends on the nucleation process and on the geometry of the crystals. K and n are respectively determined by the intercept and the slope of the straight line obtained in the plot of $\ln[-\ln(1-X_\text{t})]$ versus $\ln(t-t_0)$ (Avrami plot).

The double logarithmic Avrami plot for $PPCHD_{90}$ and $PBCHD_{90}$ samples shows a good

linearity from the beginning to the end of the crystallization. This result can be interpreted as the achievement of the highest possible level of crystal perfection under the crystallization conditions used. Such an interpretation is in agreement with the observed capability of the samples at high trans content to attain a great crystal perfection.

As regards the crystallization mechanism, it is useful to analyze the Avrami exponent. $PBCHD_{90}$ presents *n* values between 2.6–3.0 (Table 4) whereas lower values, between 2.3 and 2.4, have been found for $PPCHD_{90}$. *n* data around 2.5–3.5 are typical of heterogeneous nucleation and three-dimensional growth, whereas *n* data lower than 2.5 can be justified by the consideration that the Avrami theory describes only approximately the formation of crystals with large amounts of defects and with peculiar morphologies [46].

Crystallization half-time $t_{1/2}$ is the time at which the polymer reaches a crystalline fraction equal to 0.5 and is used to compare crystallization rates. This value was obtained by subtracting the induction time t_0 that is the time span before crystallization begins at isothermal temperature.

Finally, Figure 10 describes the trend of $1/t_{1/2}$ (which is proportional to the crystallization rate) as a function of the undercooling $\Delta T = T\text{m}^\circ - T\text{c}$ for the $PxCHD_{90}$ samples. Only a portion of the expected bell-shaped curve is obtained for each sample, in particular the part of the curve at "low" ΔT or "high" *T*c, characterized by a nucleation controlled character.

Figure 10 clearly indicates that the crystallization rate of the PxCHD samples is strongly dependent on the diol chain length and increases by increasing the number of methylene units in the diol. Indeed, the macromolecular chain becomes more flexibile and the formation of crystals by chain folding is favored.

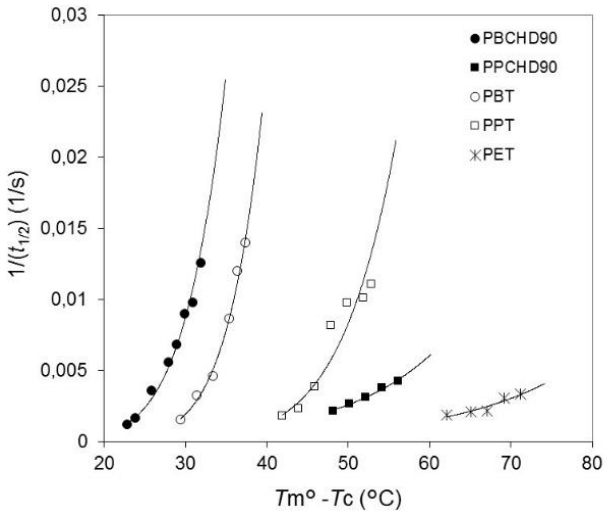

Figure 10. Semicrystallization time as a function of the undercooling for $PxCHD_{90}$ and PxT samples.

By observing the crystallization rate of the aromatic polyesters, it is notable that also in this case the crystallization rate increases from PET to PPT and then PBT, according to kinetic crystallizability parameters and energy barriers for crystallization process [47].

Finally, by comparing crystallization rates of aliphatic and aromatic samples, it results that PET and PPT crystallize faster than $PECHD_{90}$ and $PPCHD_{90}$ respectively whereas PBT crystallizes slower

than $PBCHD_{90}$. A possible explanation of this behaviour can be probably found by considering the different crystalline phases involved and a more in depth analysis in this field is necessary.

3.5. Mechanical properties

Figure 11 shows the dynamical mechanical spectrum of the $PxCHD_{90}$ samples. In the temperature range from −120 to 150 °C the $PBCHD_{90}$ sample exhibits three relaxation peaks of tan δ, denoted as γ, β and α in order of increasing temperature, according to previous results [17]. $PPCHD_{90}$ and $PECHD_{90}$ show only two relaxation peaks (β and α) in this range of temperatures.

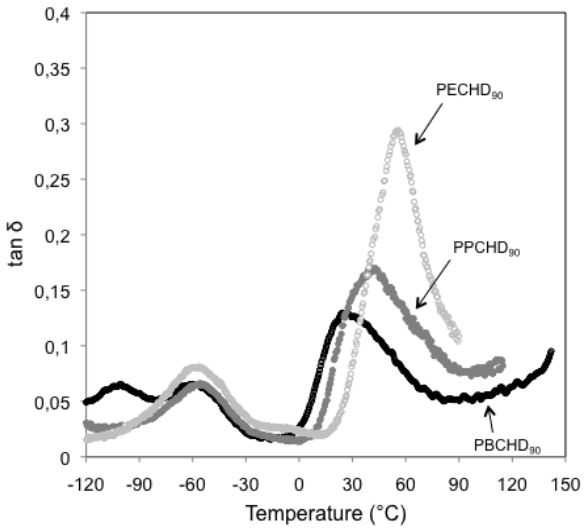

Figure 11. DMTA spectra of $PxCHD_{90}$ samples.

As regards the assignments of the observed relaxations, the α peak is assigned to the glass-to-rubber transition. From Figure 11 it is evident that these peaks shift to lower temperatures from $PECHD_{90}$ to $PBCHD_{90}$ due to a larger flexibility of a longer methylene sequence, according to the DSC results. Moreover, the intensity of the α peaks decreases from PECHD to PBCHD with the decrement of the amorphous phase amount.

As reported in [17], the β relaxation is due to the molecular motion of the cyclohexylene ring and the stereochemistry of the aliphatic ring influences the temperature of the peaks. In this case the three analyzed samples have the same percentage of trans isomer and the temperatures of the β relaxation are very close (about −60 °C).

The γ relaxation observed at about −100 °C for $PBCHD_{90}$ sample may be associated with the motions of the $-O-(CH_2)_4-O-$ units, likewise to the behavior of PBT (−80 °C) [17]. This relaxation has been studied in ref 17 and seems to depend on the amorphous amount: intensity and temperature of the peak decrease with the increment of the cis content and, then, with the increment of the amourphous phase amount. Therefore, the loss of the γ relaxation in the $PPCHD_{90}$ and $PECHD_{90}$ samples could be due to the fact that this process occurs at very low temperatures and with reduced intensity.

4. Conclusion

The solid state properties of alicyclic polyesters, characterized by the presence of the 1,4-cyclohexylene units, have been analyzed and correlated to their structure. In particular, the stoichiometry of the aliphatic ring and the length of the CH_2 sequences have been taken into consideration.

The results obtained can be summarized as follows:

- Polymers rich in trans isomer are semicrystalline, whereas polymers rich in cis isomer are amorphous: indeed, the ring in cis configuration cause kinks and disturbances in the crystal formation. The exception is represented by $PECHD_{90}$, which crystallizes with extremely slow rate, probably due to a high rigidity of the chains.
- The glass transition temperature decreases with the lengthening of the chain, due to the increment of chain flexibility.
- With respect to PET, PPT and PBT, the presence of the 1,4-cyclohexylene units, instead of aromatic rings, leads to lower transition temperatures but keep the same thermal stability.
- The crystalline phases of $PxCHD_{90}$ samples changes as a function of the length of the diol.
- The crystallization kinetic data, obtained by the Avrami equation, suggest that the crystallization of $PBCHD_{90}$ and $PPCHD_{90}$ occurs with a heterogeneous nucleation process and a three dimensional growth, independently of the number of carbons in the diol. The crystallization rate significantly increases with the increment of the number of the methylene units in the diols.

As a conclusion, tunable properties can be easily obtained by varying stereochemistry and chain length of the diol in $PxCHD_y$ samples. This good property is associated to positive mechanical performance and a potential biodegradability.

Conflict of interest

All authors declare no conflicts of interest in this paper.

References

1. Gandini A, Lacerda TM (2015) From monomers to polymers from renewable resources : Recent advances. *Prog Polym Sci* 48: 1-39.
2. Reddya MM, Vivekanandhana S, Misra M, et al. (2013) Biobased plastics and bionanocomposites: Current status and future opportunities. *Prog Polym Sci* 38: 1653-1689.
3. Miller SA (2013) Sustainable polymers: opportunities for the next decade. *ACS Macro Letters* 2: 550-554.
4. Tschan MJL, Brule E, Haquette P, et al. (2013) Synthesis of biodegradable polymers from renewable resources. *Polym Chem* 3: 836-851.
5. PlasticsEurope, available from: http://www.plasticseurope.org.
6. Sheldon R (2014) Green and sustainable manufacture of chemicals from biomass: state of the art. *Green Chem* 16: 950-963.
7. Colonna M, Berti C, Fiorini M, et al. (2011) Synthesis and radiocarbon evidence of terephthalate polyesters completely prepared from renewable resources. *Green Chem* 12: 2543-2548.

8. Gandini A, Silvestre AJD, Neto CP, et al. (2009) The furan counterpart of poly(ethylene terephthalate): an alternative material based on renewable resources. *J Polym Sci: Part A: Polym Chem* 47: 295-298.
9. Zhu J, Cai J, Xie W, at al. (2013) Poly(butylene 2,5-furan dicarboxylate), a biobased alternative to PBT: synthesis, physical properties, and crystal structure. *Macromol* 46: 796-804.
10. Fache M, Boutevin B, Caillol S (2015) Vanillin, a key-intermediate of biobased polymers. *Europ Polym J* 68: 488-502.
11. Mialon L, Pemba AG, Miller SA (2010) Biorenewable polyethylene terephthalate mimics derived from lignin and acetic acid. *Green Chem* 12: 1704-1706.
12. Wilsens CHRM, Noordover BAJ, Rastogi S (2014) Aromatic thermotropic polyesters based on 2,5-furandicarboxylic acid and vanillic acid. *Polymer* 55: 2432-2439.
13. Berti C, Binassi E, Colonna M, et al. (2010) Biobased terephthalate polyesters. US 20100168461.
14. Berti C, Celli A, Marchese P, et al. (2009) Novel copolyesters based on poly(alkylene dicarboxylate)s: 2. Thermal behavior and biodegradation of fully aliphatic random copolymers containing 1,4-cyclohexylene rings. *Eur Polym J* 45: 2402-2412.
15. Berti C, Celli A, Marchese P, et al. (2008) Novel copolyesters based on poly(alkylene dicarboxylate)s: 1. Thermal behavior and biodegradation of aliphatic-aromatic random copolymers. *Eur Polym J* 44: 3650-3661.
16. Tsai Y, Jheng LC, Hung CY (2010) Synthesis, properties and enzymatic hydrolysis of biodegradable alicyclic/aliphatic copolyesters based on 1,3/1,4-cyclohexanedimethanol. *Polym Degrad Stab* 95: 72-78.
17. Berti C, Celli A, Marchese P, et al. (2008) Influence of molecular structure and stereochemistry of the 1,4-cyclohexylene ring on thermal and mechanical behavior of poly(butylene 1,4-cyclohexanedicarboxylate). *Macromol Chem Phys* 209: 1333-1344.
18. Berti C, Binassi E, Celli A, et al. (2008) Poly(1,4-cyclohexylenedimethylene 1,4-cyclohexanedicarboxylate): influence of stereochemistry of 1,4-cyclohexylene units on thermal properties. *J Polym Sci: Part B: Polym Phys* 46: 619-630.
19. Celli A, Marchese P, Sullalti S, et al. (2011) Eco-friendly poly(butylene 1,4-cyclohexanedicarboxylate): relationships between stereochemistry and crystallization behavior. *Macromol Chem Phys* 212: 1524-1534.
20. Celli A, Marchese P, Sullalti S, et al. (2012) Bio-based (co)polyesters containing 1,4-cyclohexylene units: correlations between stereochemistry and phase behavior. In: Bradley EO, Lane MI, Editors, *New Developments in Polymers Research*. New York: Nova Science Publishers, 63-101.
21. Zhang B, Turner SR (2013) New poly(arylene ether sulfone)s based on 4,4′-[*trans*-1,4-cyclohexanediylbis(methylene)] bisphenol. *Polymer* 54: 4493-4500.
22. Zhang B, Turner SR (2011) Synthesis and Characterization of Poly(arylene ether sulfone)s with trans-1,4-Cyclohexylene Ring Containing Ester Linkages. *J Polym Sci: Part A: Polym Chem* 49: 4316-4324.
23. Yoon WJ, Oh KS, Koo JM, et al. (2013) Advanced polymerization and properties of biobased high Tg polyester of isosorbide and 1,4-cyclohexanedicarboxylic acid through in situ acetylation. *Macromol* 46: 2930-2940.
24. Chen T, Zhang J (2015) Non-isothermal cold crystallization kinetics of poly(ethylene

glycol-co-1,4-cyclohexanedimethanol terephthalate) (PETG) copolyesters with different compositions. *Polym Testing* 48: 23-30.
25. Finelli L, Lorenzetti C, Messori M, et al. (2004) Comparison between titanium tetrabutoxide and a new commercial titanium dioxide based catalyst used for the synthesis of poly(ethylene terephthalate). *J Appl Polym Sci* 92: 1887-1892.
26. Berti C, Bonora V, Colonna M, et al. (2003) Effect of carboxyl end groups content on the thermal and electrical properties of poly(propylene terephthalate). *Eur Polym J* 39: 1595-1601.
27. Pilati F (1989) Polyesters, In: Allen, G., Bevington, J.C. Editors, *Comprehensive Polymer Science*, 1 Eds., Oxford: Pergamon Press, 308.
28. Fakirov S, Seganov I, Kurdowa E (1981) Effect of chain composition of poly(ethylene terephthalate) structure and properties. *Makromol Chem* 182: 185-197.
29. Yu T, Bu H, Chen J, et al. (1986) The effect of units derived from diethylene glycol on crystallization kinetics of poly(ethylene terephthalate). *Makromol Chem* 187: 2697-709.
30. Colonna M, Berti C, Binassi E, et al. (2011) Poly(cyclohexylenedimethylene-1,4cyclohexanedicarboxylate): analysis of parameters affecting polymerization and cis-trans isomerization. *Polym Int* 60: 1607-1613.
31. Commereuc S, Lacoste J (1997) Photo- and thermo-oxidation of polyoctenamer. Photostability of hydroperoxides. *Polym Degrad Stab* 57: 31-41.
32. Wang L, Xie Z, Bi X, et al. (2006) Preparation and characterization of aliphatic/aromatic copolyesters based on 1,4-cyclohexanedicarboxylic acid. *Polym Degrad Stab* 91: 2220-2228.
33. Celli A, Marchese P, Sisti L, et al. (2013) Effect of 1,4-cyclohexylene units on thermal properties of poly(1,4-cyclohexylenedimethylene adipate) and similar aliphatic polyesters. *Polym Int* 62: 1210-1217.
34. Ki HC, Ok Park O (2001) Synthesis, characterization and biodegradability of the biodegradable aliphatic-aromatic random copolyesters. *Polymer* 42: 1849-1861.
35. Kelsey DR, Kiibler KS, Tutunjian PN (2005) Thermal stability of poly(trimethylene terephthalate). *Polymer* 46: 8937-8946.
36. Tonelli AE (1973) Effect of the terephthaloyl residue on chain flexibility of poly(ethylene terephthalate). *J Polym Sci Polym Lett Ed* 11: 441-447.
37. Tonelli AE (2002) Conformational characteristics of Poly(ethylene phthalate)s. *J Polym Sci Polym Phys* 40: 1254-1260.
38. Gonzalez CC, Riande E, Bello A, et al. (1988) Conformational characteristics of polyesters ased on terephthalic acid with an ether group in the glicol residue. *Macromolecules* 21: 3230-3234.
39. Sandhya TE, Ramesh C, Sivaram S (2007) Copolyesters based on poly(butylene terephthalate)s containing cyclohexyl and cyclopentyl ring: effect of molecular structure on thermal and crystallization behaviour. *Macromolecules* 40: 6906-6915.
40. Wunderlich B (1980) Crystal Melting, In: Wunderlich, B. Author, *Macromolecular Physics*, New York: Academic Press.
41. Hoffman JD, Weeks JJ (1962) Melting process and equilibrium melting temperature of poly(chlorotrifluoroethylene). *J Res Natl Bur Stand* 66A: 13-28.
42. Chisolm BJ, Zimmer JG (2000) Isothermal crystallization kinetics of commercially important polyalkylene terephthalates. *J Appl Polym Sci* 76: 1296-1307.
43. Avrami M (1939) Kinetics of phase change. I. General theory. *J Chem Phys* 7: 1103-1112.

44. Avrami M (1940) Kinetics of phase change. II. Transformation-time relations for random distribution of nuclei. *J Chem Phys* 8: 212-224.
45. Avrami M (1941) Granulation, phase change and microstructure. Kinetics of phase change. III. *J Chem Phys* 9: 177-184.
46. Wunderlich B (1976) Crystal Nucleation, Growth, Annealing, In: Wunderlich, B. Author, *Macromolecular Physics*, New York: Academic Press.
47. Dangseeyun N, Srimoaon P, Supaphol P, et al. (2004) Isothermal melt-crystallization and melting behavior for three linear aromatic polyesters. *Thermochimica Acta* 409: 63-77.

AIMS Press